Microsc. Microanal. 19, 693–697, 2013
doi:10.1017/S1431927613000445

Microscopy AND Microanalysis

Automatic Crystallographic Characterization in a Transmission Electron Microscope: Applications to Twinning Induced Plasticity Steels and Al Thin Films

M. Galceran,[1,3,*] A. Albou,[2] K. Renard,[2] M. Coulombier,[2] P.J. Jacques,[2] and S. Godet[1]

[1]*4MAT (Materials Engineering, Characterization, Synthesis and Recycling), Université Libre de Bruxelles, Avenue F.D. Roosevelt 50, 1050 Brussels, Belgium*
[2]*Université catholique de Louvain, Institute of Mechanics, Materials and Civil Engineering, IMAP, Place Sainte Barbe 2, B-1348 Louvain-la-Neuve, Belgium*
[3]*CIC Energigune, Albert Einstein 48, 01510 Miñano (Álava), Spain*

Abstract: A new automated crystallographic orientation mapping tool in a transmission electron microscope technique, which is based on pattern matching between every acquired electron diffraction pattern and precalculated templates, has been used for the microstructural characterization of nondeformed and deformed aluminum thin films and twinning-induced plasticity steels. The increased spatial resolution and the use of electron diffraction patterns rather than Kikuchi lines make this tool very appropriate to characterize fine grained and deformed microstructures.

Key words: twinning, thin films, transmission electron microscopy, electron diffraction, orientation mapping

Introduction

Since the 1980s, the local crystallography of materials can be studied in an automated way thanks to electron backscattered diffraction (EBSD) techniques in a scanning electron microscope (SEM). This technique relies on the indexation of the Kikuchi patterns recorded on a phosphorous screen inside the SEM chamber. Spatial resolution of a few tens of nanometers (typically 50 nm) can be reached together with an angular resolution of about 1° in the case of field emission gun SEM (FEG-SEM) (Humphreys et al., 1999). The use of these techniques led to significant advances in the field of materials science thanks to the combination of diffraction and imaging. Among others, the characterization of local textures, the concept of grain boundary engineering (Randle, 1999; Randle & Owen, 2006), the analysis of the crystallography of phase transformations at the scale of individual parent grains (Godet et al., 2004; Lambert-Perlade et al., 2004; Gourgues-Lorenzon, 2009), and new insights into the mechanisms leading to the formation of deformed microstructures, such as grain fragmentation or the building up of orientation gradients (Mizera & Driver, 1999; Delannay et al., 2001), benefited from the development of the EBSD techniques.

Although EBSD is now a mature technique for the characterization of the local crystallography in many studies, further developments may suffer from incompatibilities between the actual resolution levels and the scale of the investigated phenomena. Indeed, spatial resolution can be a limitation in the characterization of finely grained materials with sizes well below 1 μm. Furthermore, SEM-EBSD is not well suited for the characterization of severely deformed microstructures because it is well known that the presence of dislocations leads to weak or blurred Kikuchi patterns hindering their indexation and thus deteriorating the indexing rate. Finally, it is worth noting that EBSD requires a minimum (backscattering) volume of materials, especially for materials having a low backscattered cross section. A nonexhaustive list of topics for which EBSD with improved capabilities would be useful is:

1. The continuous improvement of the strength/ductility balance of new alloys by combining dislocation glide with other deformation mechanisms such as mechanically-induced phase transformations (Grassel et al., 2000) or mechanical twinning (Allain et al., 2004; Idrissi et al., 2010*a*; Marteleur et al., 2012). These deformation mechanisms bring about complex microstructures that must be characterized at a scale well below the initial grain size of the material.
2. The miniaturization of devices such as micro- and nano-electromechanical systems. In these systems, it is impossible to correct a defect during service so that their durability can only be ensured by a thorough understanding of the deformation mechanisms at very small scales (Spearing, 2000).
3. The development of functional thin films or coatings with ductility properties that allow forming applications to be conducted on the sheet after the deposition of the film (Evans & Hutchinson, 2008; Brugger et al., 2010).

In recent years, Rauch and co-workers (Rauch & Veron, 2005) developed a new tool enabling automated crystallographic orientation mapping in a transmission electron microscope (ACOM-TEM). Instead of using Kikuchi patterns for the determination of the local orientations, ACOM-TEM is based on electron diffraction (ED) pattern matching.

Received October 15, 2012; accepted January 28, 2013
*Corresponding author. E-mail: mgalcera@ulb.ac.be

A selected area is scanned, and the electron diffraction patterns are collected with an external charge-coupled device (CCD) camera. Every acquired ED pattern is then stored in a computer and compared (off-line) to the precalculated templates, and the best match is selected. Thanks to the use of the ED patterns, this technique is insensitive to the presence of dislocations and therefore well-suited for severely deformed samples. Moreover, a spatial resolution around 1 nm can be obtained for FEG-TEM. It is rather straightforward to note that samples for the ACOM-TEM analysis should be thin enough as to present only one grain in the thickness. The presence of multiple orientations within the specimen thickness makes the pattern matching procedure very difficult if not impossible.

It has to be noted that the pattern matching procedure always leads to the selection of one of the precalculated orientations. This is quite different from conventional EBSD techniques, for which pixels can be nonindexed. To provide further information about the matching quality, this technique also provides two parameters: namely the correlation index and the reliability (these parameters can thus be compared to index quality and confidence index in conventional EBSD techniques, respectively). The highest value of the correlation index corresponds to the best match between the experimental ED pattern and the selected ED template. The reliability parameter provides a quantitative measure regarding how confident one can be regarding the matching. Indeed, it compares the quality of indexation for the best and second best matches. A low reliability value means that there is more than one possible solution, and a high reliability value is obtained when the best solution has a correlation index significantly larger than the next possible solution. An important example is the so-called "180° ambiguity" (Rauch & Veron, 2005). It arises with diffraction spots in the zero order Laue zone, which can be indexed as (hkl) or $(\text{-}h\text{-}k\text{-}l)$. Those pixels are plotted in the reliability map as a black area.

This article aims to illustrate the advantages of the ACOM-TEM technique for the analysis of local crystallographic orientation mapping in different microstructures that are difficult to characterize using conventional EBSD techniques. It focuses on strained aluminum thin films (Coulombier et al., 2010) and twinning-induced plasticity (TWIP) steels for which a large strength-ductility balance results from the formation of nanoscopic mechanical twins. Further outcomes of the use of the ACOM-TEM technique for the characterization of the TWIP effect can be found in Albou et al. (2013).

Materials and Methods

The experimental measurements were carried out using a Philips CM20 (Philips, Guildford, Surrey, UK) operating at 200 kV and equipped with a LaB_6 gun and an external source device, DigiSTAR® developed by NanoMEGAS (www.nanomegas.com), that enables the precession of the beam and substantially improves the quality of the collected ED patterns. In the precession mode (PED), proposed by Vincent and Midgley (1994), the incident beam is precessed in a hollow cone surface as the data are collected. This leads to a large improvement in the quality of ED patterns by reducing dynamical effects, observed for example in the case of thickness increase. In that case, the ED patterns present a strong diffuse inelastic scattering background with Kikuchi lines and a reduced number of ED spots. The PED mode increases the number of ED spot patterns in the reciprocal space and avoids the formation of Kikuchi lines. Consequently, there is a larger template matching leading to larger values of the correlation index and fewer ambiguities. Acquisitions were carried out with spot sizes ranging from 35 to 6 nm and acquisition frequencies from 40 to 170 frames per second using an external CCD camera. A typical map is usually collected in 15 min up to 1 h for large areas. The ASTAR® software was used for the on-line data acquisition, the generation of the templates with a predefined angular resolution, and the data treatment. Beside the conventional crystallographic tools such as the inverse pole figure imaging, it was possible to build virtual bright-field (VBF) and virtual dark-field (VDF) images by using a virtual diaphragm of predefined opening centered either on the transmitted beam or on a specific diffraction spot.

Results and Discussion

Nondeformed and Deformed Aluminum Thin Films

Aluminum thin films with a thickness of 375 nm were prepared by sputtering at a temperature around 150°C. Details about the processing stages can be found in Coulombier et al. (2010). Figure 1a shows a conventional EBSD orientation map using a step size of 35 nm of this sample. As mentioned in the introduction, the poor quality of the map can be attributed to the weakness of the backscattered signal. Indeed, the film was 375 μm and has a low backscattered cross section. The same sample was characterized by ACOM-TEM (Fig. 1b). The sample was transferred onto a TEM grid using a Quanta 3D SEM (FEI Company, Hillsboro, OR, USA) equipped with a focused ion beam (FIB). The micrograph is 350×350 pixels in size and was obtained using a step size of 20 nm with an acquisition frequency of 163 fps. It is clearly observed that the ACOM-TEM technique allows a better indexation to be obtained. This is mainly related to the fact that it is not limited by the backscattered cross section of the sample. Moreover, as it can be seen from the {111} pole figure extracted from the ACOM-TEM data, it is found that the film exhibits a $\langle 111 \rangle$//ND fiber texture. The mean grain size that can be easily calculated based on a grain boundary misorientation definition of 15° is about 350 nm. This is close to the thickness of the film, which is typical of columnar structures. It must be stressed that no cleaning procedure has been used for this specimen. As already mentioned, all the pixels are indexed at the end of the pattern matching procedure.

The samples were strained using an "on-chip" laboratory concept developed in Gravier et al. (2009). The de-

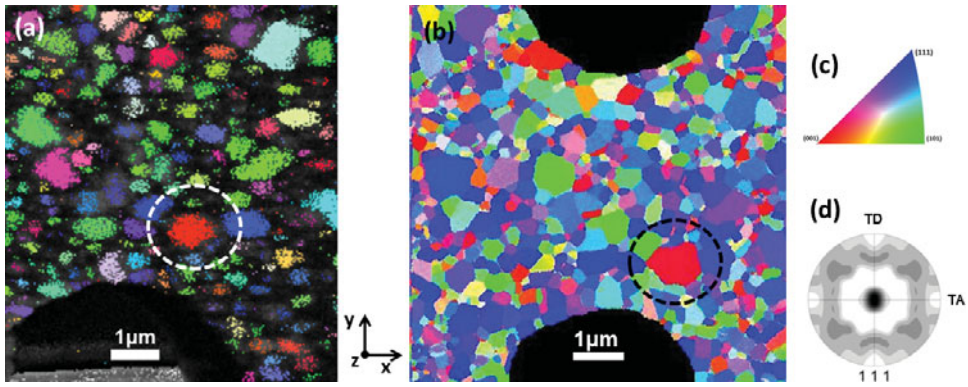

Figure 1. (**a**) Conventional EBSD orientation map, (**b**) ACOM-TEM orientation map of the as-deposited aluminum thin film, (**c**) inverse pole figure coloring code, and (**d**) {111} pole figure extracted from the ACOM-TEM data

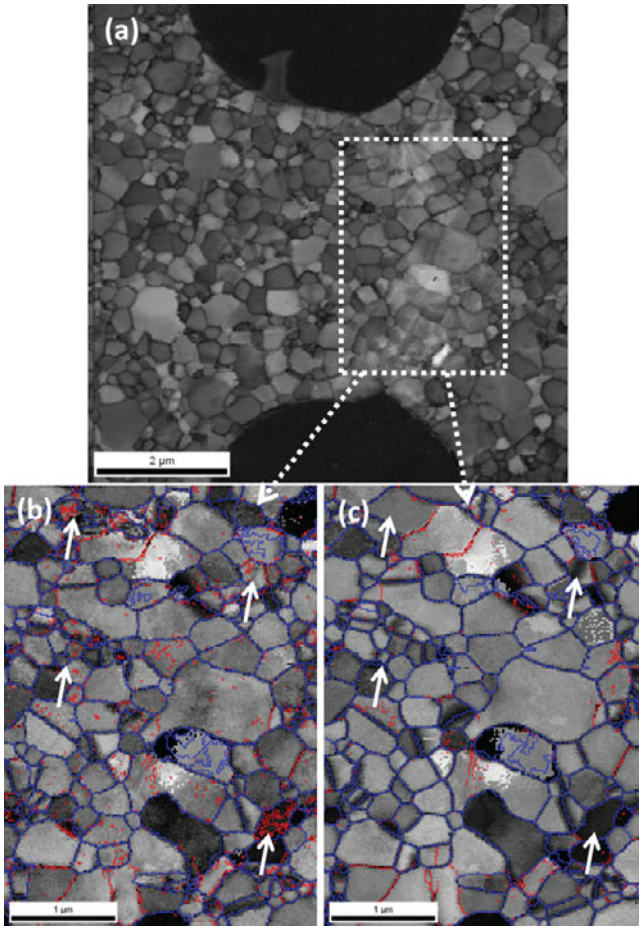

Figure 2. (**a**) Index map of deformed aluminum thin film; (**b**, **c**) reliability map of the necking area without and with PED mode, respectively. Low (red) and high (blue) angle boundaries are plotted.

formed samples were typically of the order of 6 μm in width and 50 μm in length. The localization of the deformation was ensured by the use of notched samples. After deformation, the sample was machined and transferred onto a TEM grid using a FIB and studied using the ACOM-TEM technique. The deformation did not lead to a decrease in the quality of the indexation. The microstructure presents

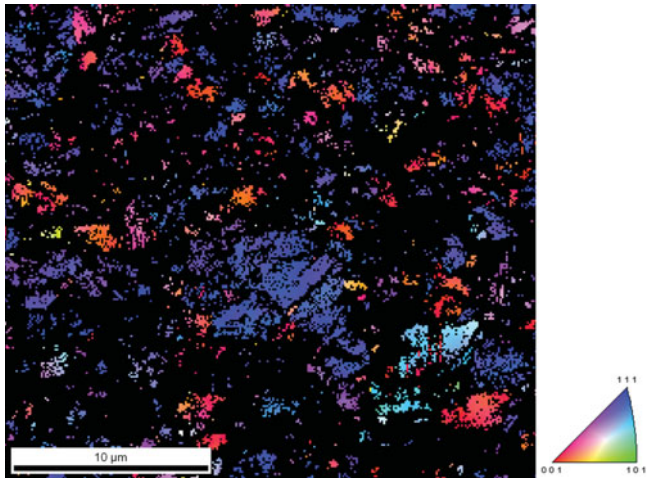

Figure 3. A typical EBSD orientation map of TWIP steel with a strain level of $\varepsilon = 0.4$. The poor quality of the orientation map is due to the presence of dislocations leading to blurred Kikuchi patterns.

a necking region, which is thinner and leads to higher index values than the rest of the sample (Fig. 2a). The PED mode with a precession angle of 1.5° was used to further enhance the quality of the indexation. Precession enabled the maximum value of the correlation to be increased by 25% (from 1200 to 1500). Of even more interest is the comparison between the reliability maps with and without precession of Figures 2b and 2c, respectively. It is observed that the number of low angles boundaries ($<2°$, in red in Figs. 2b, 2c) decreases drastically (by 50%) when the precession mode is used. A vast majority of the grains exhibit very good reliability as it can be seen from the reliability map, analogous to the EBSD-SEM confidence index, which clearly reveals grain boundaries and the microstructure. The arrows plotted on Figures 2b and 2c highlight different grains for which the use of the PED mode led to a clear improvement of the indexation. The number of low angle boundaries decreases in the PED mode from 51.7 μm to 24.3 μm in length. Consequently, the identification through the template matching will be of a higher fidelity, and this may be used to improve the quality of the orientation maps. This

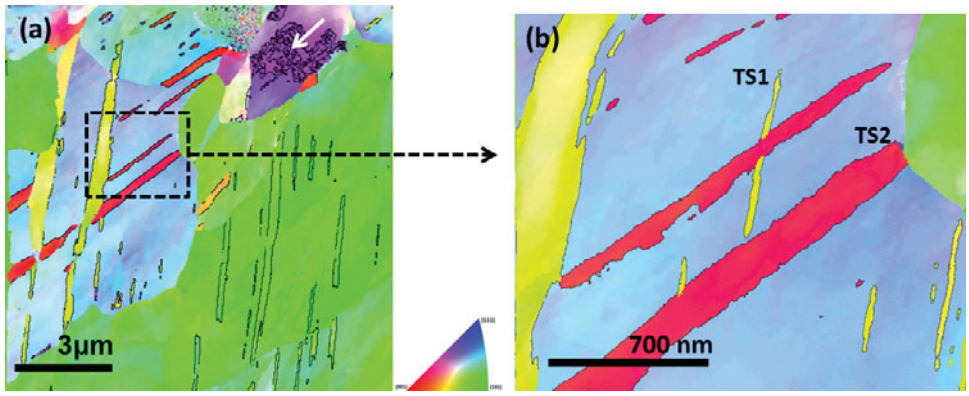

Figure 4. ACOM-TEM orientation maps of the TWIP steel investigated (**a**) 400 × 400 pixels with a step size of 20 nm (the white arrow shows the purple grain) and (**b**) 500 × 420 pixels with a step size of 4 nm. Inverse pole figure coloring code (inset). Twin system 1 (TS1) and twin system 2 (TS2)

means that the precession mode allows a reduction of the noise level (increases the accuracy of the indexation). It has to be noted that the number of grains exhibiting ambiguities (high angle boundaries >15° in blue) was not affected by the precession mode. This could be attributed to the high symmetry of the FCC structure of Al that makes it less sensitive to the precession mode compared to low symmetry crystals such as the one studied in Rauch et al. (2008).

Austenitic TWIP Steel

A TWIP steel (Fe-20%Mn-1.2%C, cubic system with space group Fm3m) with a grain size around 3 μm deformed to a true strain of $\varepsilon = 0.4$ in tension was also studied. After tensile testing, these specimens were conventionally prepared using electropolishing followed by twin-jet electropolishing with a solution of 5% $HClO_4$ and 95% acetic acid at a temperature of 12°C (Idrissi et al., 2010*b*). A typical EBSD scan of this material is presented in Figure 3. Due to the large amount of deformation defects (dislocations, etc.), the Kikuchi patterns are more and more blurred, leading to a drastic decrease of the indexing level. SEM-EBSD is thus not well suited for the characterization of severely deformed microstructures.

The ACOM-TEM technique was used on the same sample. A global view of the sample containing twins is given in Figure 4a, where an orientation map (400 × 400 pixels) obtained using a step size of 20 nm (acquisition time and acquisition frequency of 15 min and 163 fps, respectively) is shown. Although the size of the area scanned is much smaller than what can be obtained by the EBSD technique, it is clear that the quality of the indexation is not altered by the deformation and that the twins and the twin/matrix interfaces can be indexed. The data presented here are raw data, and no cleaning procedure has been applied. As a consequence some ambiguities are visible in the "purple grain" (close to [112]//ND, white arrow in Fig. 4), which is known to be very sensitive to this effect. It can be seen that two twinning systems have been activated. A small area, 500 × 420 pixels, in the same region has been

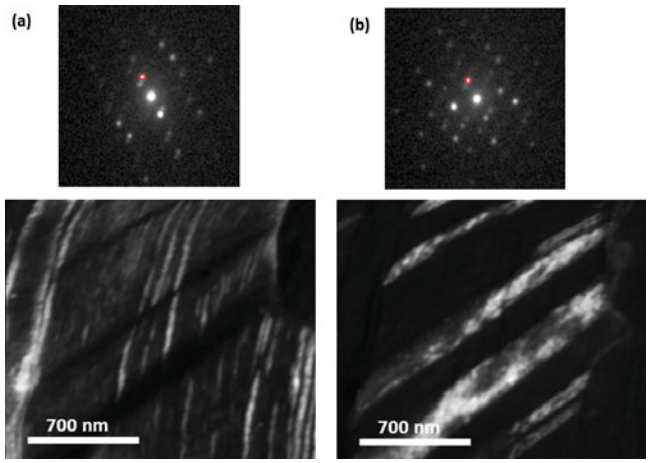

Figure 5. VDF images of the two twin families in the orientation map of Figure 4b.

scanned using the smallest spot size, 6 nm, and a step size of 4 nm. This is presented in Figure 4b, corresponding to an acquisition time of 50 min at an acquisition frequency of 67 fps. It is evident that, although the deformation level is quite large and the grains are small, the quality of the indexation is preserved. By increasing the spatial resolution (from 20 nm to 4 nm in step size), an increase in the resolution can be observed in both twin systems in more details. In the case of the twin system 1 (TS1), refining the step size allowed additional twins to be revealed. The twinning systems exhibit the traditional crystallographic relationship 60°⟨111⟩ misorientation with respect to the matrix. It has to be noted that this orientation relationship seems to be preserved even at large strain levels. A more detailed study of the crystallographic features of mechanical twinning in this steel can be found in Albou et al. (2013). In Figure 5, the two twin systems of Figure 4b have been highlighted by using the VDF mode. They are obtained with the ASTAR software using a virtual aperture (red circle in the ED patterns) around a particular reflection spot in the ED pattern. It can be considered as a possible way of quantifying the twin volume fraction.

Conclusions

ACOM-TEM is an important newly-developed technique that allows studying the characteristics of fine grain materials, deformed structures, and materials with low backscattered cross sections with high resolution, fast acquisition time, and data treatment. Also, the technique presents several off-line tools such as VBF, VDF images, and orientation and phase maps that allow an in-depth and straightforward characterization of the microstructure. It also presents some limitations with respect to the conventional EBSD techniques such as the limited size of the scanned area and the necessity that the samples be thin enough as to present only one grain through the thickness. Conventional EBSD analyses cannot provide such accurate characterization of the interfaces (grain and twin boundaries) because the spatial resolution is larger (by about 10 times). As a consequence, ACOM-TEM and EBSD techniques should be considered as complementary tools for the microstructural characterization of engineering materials.

Acknowledgments

This work was supported by the financial support of the Walloon Region through the First Postdoc programme. The financial support of the Fonds National de La Recherche Scientifique is also acknowledged. The authors are indebted to Suzanne De Kegel and Didier Robert for the sample preparation. Part of this work was carried out in the framework of the Interuniversity Attraction Poles program of the Belgian State Federal Office for Scientific, Technical and Cultural Affairs, under Contract No. P7/21.

References

Albou, A., Galceran, M., Renard, K., Godet, S. & Jacques, P.J. (2013). Nanoscale characterization of the evolution of the twin–matrix orientation in Fe–Mn–C twinning-induced plasticity steel by means of transmission electron microscopy orientation mapping. *Scripta Mater* **68**, 400–403.

Allain, S., Chateau, J.P. & Bouaziz, O. (2004). A physical model of the twinning-induced plasticity effect in a high manganese austenitic steel. *Mater Sci Eng A* **387–389**, 143–147.

Brugger, C., Coulobier, M., Massart, T.J., Raskin, J.P. & Pardoen, T. (2010). Strain gradient plasticity analysis of the strength and ductility of thin metallic films using an enriched interface model. *Acta Mater* **58**, 4940–4949.

Coulombier, M., Boé, A., Brugger, C., Raskin, J.P. & Pardoen, T. (2010). Imperfection-sensitive ductility of aluminium thin films. *Scripta Mater* **62**, 742–745.

Delannay, L., Mishin, O.V., Juul Jensen, D. & Van Houtte, P. (2001). Quantitative analysis of grain subdivision in cold rolled aluminium. *Acta Mater* **49**, 2441–2451.

Evans, A.G. & Hutchinson, J.W. (2008). The thermomechanical integrity of thin films and multilayers. *Acta Mater* **43**, 2507–2530.

Godet, S., Glez, J.C., He, Y., Jonas, J.J. & Jacques, P.J. (2004). Grain-scale characterization of transformation textures. *J Appl Crystallogr* **37**, 417–425.

Gourgues-Lorenzon, A.F. (2009). Application of electron backscatter diffraction to the study of phase transformations: Present and possible future. *J Microsc* **233**, 460–473.

Grassel, O., Krüger, L., Frommeyer, G. & Meyer, L.W. (2000). High strength Fe-Mn-(Al, Si) TRIP/TWIP steels development—properties—application. *Int J Plast* **16**, 1391–1409.

Gravier, S., Coulombier, M., Safi, A., André, N., Boé, A., Raskin, J.P. & Pardoen, T. (2009). New MEMS-based micromechanical testing laboratory—Application to aluminium, polysilicon and silicon nitride. *J Microelectromech Syst* **18**, 555–565.

Humphreys, F.J., Huang, Y., Brough, I. & Harries, C. (1999). Electron backscatter diffraction of grain and subgrain structures—Resolution considerations. *J Microsc* **195**, 212–216.

Idrissi, H., Renard, K., Ryelandt, L., Schryvers, D. & Jacques, P.J. (2010*a*). On the mechanism of twin formation in Fe-Mn-C TWIP steels. *Acta Mater* **58**, 2464–2476.

Idrissi, H., Ryelandt, L., Schreyvers, D. & Jacques, P.J. (2010*b*). On the relationship between the twin internal structure and the work-hardening rate of TWIP steels. *Scripta Mater* **63**, 961–964.

Lambert-Perlade, A., Gourgues, A.F. & Pineau, A. (2004). Austenite to bainite phase transformation in the heat-affected zone of a high strength low alloy steel. *Acta Mater* **52**, 2337–2348.

Marteleur, M., Sun, F., Gloriant, T., Vermaut, P., Jacques, P.J. & Prima, F. (2012). On the design of new β-metastable titanium alloys with improved work hardening rate thanks to simultaneous TRIP and TWIP effects. *Scripta Mater* **66**, 749–752.

Mizera, J. & Driver, J.H. (1999). Microtexture analysis of a hot deformed Al-2.3wt.%Li-0.1wt.%Zr alloy. *Mater Sci Eng A* **271**, 334–343.

Randle, V. (1999). Menchanism of twining-induced grain boundary engineering in low stacking fault energy materials. *Acta Mater* **47**, 4187–4196.

Randle, V. & Owen, G. (2006). Mechanism of grain boundary engineering. *Acta Mater* **54**, 1777–1783.

Rauch, E.F. & Veron, M. (2005). Coupled microstructural observations and local texture measurements with an automated crystallographic orientation mapping tool attached to a TEM. *J Mater Sci Eng Tech* **36**, 552–556.

Rauch, E.F., Veron, M., Portillo, J., Bultreys, D., Maniette, Y. & Nicolopoulos, S. (2008). Automatic crystal orientation and phase mapping in TEM by precession diffraction. *Microsc Anal* **22**, S5–S8.

Spearing, S.M. (2000). Materials issues in microelectromechanical systems (MEMS). *Acta Mater* **48**, 179–196.

Vincent, R. & Midgley, P. (1994). Double conical beam-rocking system for measurement of integrated electron diffraction intensities. *Ultramicroscopy* **53**, 271–282.